NANO LETTERS

2008
Vol. 8, No. 5
1527-1531

Electric Field Quenching of Carbon Nanotube Photoluminescence

Anton V. Naumov,† Sergei M. Bachilo,‡ Dmitri A. Tsyboulski,‡ and R. Bruce Weisman*,‡

Applied Physics Program and Department of Chemistry, Richard E. Smalley Institute for Nanoscale Science and Technology, and Center for Biological and Environmental Nanotechnology, Rice University, 6100 Main Street, Houston, Texas 77005

Received January 11, 2008; Revised Manuscript Received March 20, 2008

ABSTRACT

The effect of external electric fields on the photoluminescence intensity of single-walled carbon nanotubes was investigated for individual nanotubes and bulk samples in polymeric films. Fields of up to 10^7 V/m caused dramatic, reversible decreases in emission intensity. Quenching efficiency varied as the cosine of the angle between the field and nanotube axis and decreased with increasing optical band gap. Photoluminescence intensity was found to follow a reciprocal hyperbolic cosine dependence on electric field.

Because of their outstanding mechanical, thermal, optical, and electronic properties, carbon nanotubes have recently been the focus of intense basic and applied research.[1,2] Nanotubes are already employed as probe tips in atomic force microscopy and as efficient field emission sources.[3,4] Carbon nanotubes may also form the basis for revolutionary optical and electronic nanoscale devices, such as ultrafast optical switches and next-generation field-effect transistors made from individual single-walled carbon nanotubes (SWCNTs).[5–8] In addition, some optoelectronic devices have recently been demonstrated in which individual semiconducting SWCNTs emit photoluminescence through recombination of carriers injected at the ends of the nanotube.[9] The electroluminescence of SWCNTs in a similar device geometry has also been reported.[10] The well-known structure-dependent luminescence of semiconducting SWCNTs provides a powerful tool for monitoring electronic perturbations on the nanotube induced by external fields or currents.[11] This approach was employed in the photoluminescence study of SWCNT field effect transistors, where it was found that emission intensity varied with source-drain current.[12] There is a continuing search for other applications arising from the interaction of applied fields with carbon nanotubes. The importance of such interactions has led several theoretical researchers to investigate the electronic and optical properties of metallic and semiconducting carbon nanotubes in external electric and magnetic fields.[13–17] It was predicted that applying a transverse electric field to semiconducting SWCNTs will induce changes in band gaps and affect the lifetime of electronically excited states.[13,14,16] It has also been pointed out that applied electric fields should shift the positions of optical absorption peaks and increase their number by breaking state degeneracy. Recent electroabsorption studies have detected very small ($\sim 10^{-4}$) relative changes in SWCNT absorption in high electric fields (0.1−1 MV/cm).[18,19] However, experimental studies of SWCNT excited states in external fields remain very limited. We describe here the results of single-nanotube and bulk photoluminescence studies that reveal substantial quenching of SWCNT emission in external fields. In contrast to all of the emission studies cited above, which were performed on SWCNTs in electrical circuits, the nanotubes in our research were not electrically contacted.

Samples were prepared using HiPco SWCNTs produced at Rice University.[20] These were dispersed in a 1 wt % aqueous solution of Triton-X surfactant and bath sonicated for 1 h. The resulting suspension was centrifuged at 12 000× g for 6 h, after which the top decant portion was collected. Several drops of this portion were added to approximately 8 mL of a solution of ∼5% poly(methyl methacrylate) (PMMA) in *o*-xylene, and the mixture was tip sonicated at ∼10 W power for 10 min to stimulate evaporation of the water and prevent nanotube aggregation. This gave a clear *o*-xylene solution rich in individual SWCNTs coated by PMMA and Triton-X. Two types of PMMA with molecular weights of 350 000 and 996 000 were used in these experiments; the longer-chain polymer was found to form more robust films.

Several drops of the *o*-xylene SWCNT/PMMA suspension were spin-coated onto a microscope slide with electrodes. Evaporation of the solvent left a clear, uniform PMMA film on the substrate. These films were several micrometers thick

* Corresponding author. E-mail: weisman@rice.edu.
† Applied Physics Program.
‡ Department of Chemistry.

10.1021/nl0800974 CCC: $40.75
Published on Web 04/23/2008

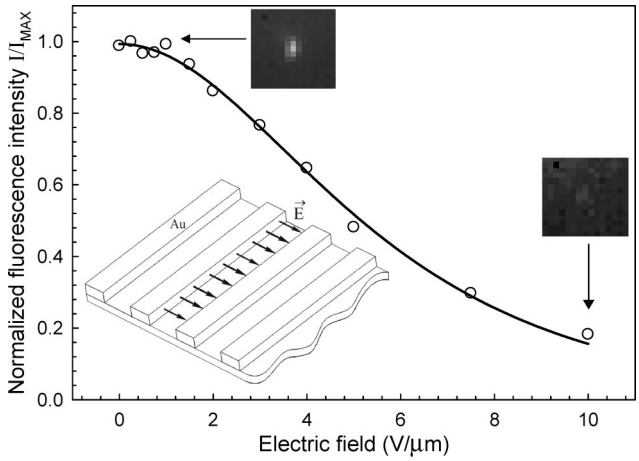

Figure 1. Dependence of the photoluminescence intensity of a single SWCNT on applied electric field. The maximum absolute intensity was ~7000 counts in a 0.5 s acquisition time. Open circles show measured data, and the solid curve is a best fit based on an inverse hyperbolic cosine function with a quenching parameter $k = 0.254$ μm/V. The lower left insert illustrates the interdigitized gold array electrodes used for these measurements. Photoluminescence images of the nanotube at 0 and 10 V/ μm are also shown.

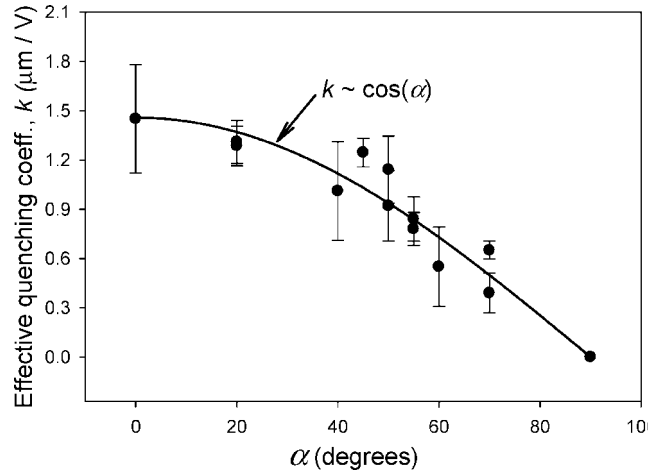

Figure 2. Dependence of effective quenching coefficient k on the angle α between SWCNT axis and electric field. Symbols show experimental data, and the solid curve is a cosine fit.

and were embedded with isolated, individual SWCNTs. Three types of electrodes were employed in the present experiments. First, we used glass microscope slides coated uniformly with a thin, highly transparent layer of indium tin oxide (ITO). The PMMA/SWCNT films were deposited on the surfaces of 2 of these slides that were then compressed together to make a parallel plate capacitor with plates separated by 15 μm of PMMA. The embedded nanotubes in this capacitor were subjected to electric fields of up to ~20 V/μm. Although occasional film samples experienced dielectric breakdown under these conditions, we could normally detect no current flow between the electrodes. A second electrode configuration consisted of a glass substrate with an array of deposited gold interdigitated electrodes (Figure 1). The electrodes were gold stripes with dimensions 20 μm wide, 3 mm long, and 1.1 μm thick. These electrodes were separated by 20 μm spaces and connected to two separate terminals. In this configuration, voltages of up to 200 V were applied to generate fields on the order of several volts per micrometer. The substrate with interdigitated electrodes was cemented to a microscope slide and spin-coated with nanotubes in PMMA to fully encapsulate the electrodes. The third electrode configuration was custom-made to allow a variation of the direction of the electric field relative to a stationary nanotube. It consisted of a substrate with 4 triangular gold electrodes oriented at 90° to each other, with gaps of about 50 μm between tips. After spin-coating SWCNTs in PMMA onto the substrate, isolated nanotubes located near the center of the electrode gap were selected for study. The direction of the electric field was then controlled by applying voltages to selected electrodes or groups of electrodes. This allowed us to rotate the field in steps of 45° while recording photoluminescence from a SWCNT.

To monitor emission intensities from individual SWCNTs located in the plane of the electrodes in the second and third configurations discussed above, we used a near-infrared (NIR) fluorescence microscope apparatus described previously.[21] In brief, this instrument excites E_{22} transitions of SWCNTs with a 785 nm diode laser. The resulting NIR E_{11} emission is collected by a 60× water or oil immersion objective of a Nikon TE-2000U inverted microscope, spectrally filtered, and directed into a Roper OMA V 2D InGaAs camera. Emission from a selected region of the sample can also be directed to a spectrograph with a Roper OMA V InGaAs array for spectral analysis. Both detectors are cryogenically cooled. This apparatus allowed the (n,m) identification of individual carbon nanotubes[22,23] and studies of their emission in controlled electric fields. A carbon nanotube is most efficiently excited by light polarized parallel to its axis. Therefore, the orientation of individual nanotubes in the plane of the film could be clearly determined by monitoring photoluminescence intensity while rotating the polarization of the excitation beam with a half-wave plate.

In addition to investigations on individual nanotubes, we also studied electric field effects on the photoluminescence of bulk carbon nanotube samples in thick PMMA films. Such samples were obtained by drying SWCNT suspensions in PMMA/xylene on a glass substrate. The concentration of SWCNTs in these films was made high enough to obtain adequate photoluminescence spectra. The dried films were placed between two semitransparent ITO electrodes. Photoluminescence was then recorded using a Spex Fluorolog 3−211 spectrofluorometer with a Xe lamp excitation source and an InGaAs single-channel detector cooled with liquid nitrogen. For some measurements, excitation was instead provided by diode lasers emitting up to 1 W at 980 nm or 0.5 W at 670 nm.

In a series of experiments, we observed that application of electric fields of several volts per micrometer caused a drastic decrease in photoluminescence intensity for many individual carbon nanotubes (Figure 1). This effect was generally found to be reproducible and reversible. The

emission intensity of most SWCNTs recovered to initial values when the external field was removed, although a minority showed slightly irreversible quenching. Photoluminescence intensity was recorded as a function of electric field strength as it was varied from zero to maximum and back to zero. Emission intensities were averaged over several measurement cycles and plotted versus electric field (Figure 1). At higher fields these quenching curves appeared approximately exponential; however, at low fields, they became nearly flat. Several simple functional fits were compared, and it was found that an inverse hyperbolic cosine function (eq 1) best described the field dependence. In such fits, a single "quenching parameter" k describes the sensitivity of nanotube photoluminescence intensity to the applied electric field. The parameter A represents the peak (zero-field) intensity, which has been normalized to 1 in Figure 1.

$$I = \frac{A}{\cosh(kE)} = \frac{2A}{\exp(kE) + \exp(-kE)} \quad (1)$$

We found that SWCNT photoluminescence quenching observed with planar ITO electrodes was significantly weaker than with interdigitated electrodes at the same field values. In the case of ITO electrodes, the photoluminescence intensity decrease was just noticeable at 3 V/μm and became significant only at ~20 V/μm, whereas with the gold interdigitated electrodes, emission quenching was substantial at 2 V/μm. A likely reason for this difference is the orientation of SWCNTs in the film relative to the electric field. During the process of spin-coating, SWCNTs tended to orient randomly in the plane parallel to the slide surface. Since the field generated using ITO electrodes was perpendicular to the surface, most SWCNTs were therefore orthogonal to the electric field vector. However, with the interdigitated electrodes, the electric field was parallel to the surface. This allowed many of the SWCNTs in the film to lie along the field vector. The extremely weak quenching observed with perpendicular fields suggests that photoluminescence quenching is dominated by electric fields parallel to the nanotube axis.

If in fact only the projection $E_{||}$ of the electric field is responsible for quenching, the coefficient k should depend on the angle α between SWCNT and the field. Then, $kE_{||} = k(E\cos(\alpha)) = (k\cos(\alpha))E$, should be used in eq 1, and the effective quenching coefficient would be $k\cos(\alpha)$. Our photoluminescence studies of carbon nanotubes randomly oriented at various measured angles confirm that the effective quenching coefficient decreases with increasing angle α. The effective quenching coefficients were found using inverse hyperbolic cosine modeling of 13 experimental runs and then plotted versus the angle between the carbon nanotube and the electric field (Figure 2). In this set, only SWCNTs fluorescing in the range from 1250 to 1400 nm were included. This wavelength selection limited the range of SWCNT diameters and decreased the influence of structural effects on the data in Figure 2.

As seen from Figure 2, $\cos(\alpha)$ appears to provide a reasonable fit to the data. However, there are noticeable deviations, suggesting that some other factors may also influence the quenching process. These may include such

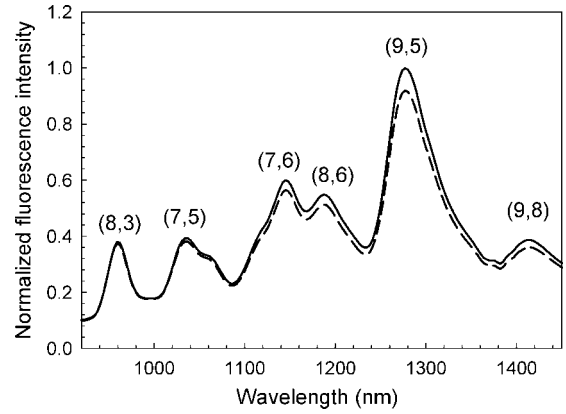

Figure 3. Photoluminescence emission spectra of SWCNTs in a PMMA film excited by a 670 nm diode laser with no applied field (solid curve) and with an external field of 2.3 V/μm (dashed curve). Major spectral peaks are labeled with their dominant (n,m) species. The spectral resolution was 3 nm.

variable SWCNT properties as chiral angle, diameter, and length, as well as defect levels. To eliminate these other factors, we studied single nanotubes in the custom-made triangular electrode structure that allowed the electric field to be rotated from 0 to 360° in 45° increments while recording their emission intensities at fixed field magnitudes. After correction for nonuniform distances from the electrodes, these data confirmed the $\cos(\alpha)$ dependence.

An important question is the dependence of electric field quenching on the SWCNT structure. To investigate this, we conducted studies on bulk SWCNT samples. This approach had several advantages over single-nanotube approaches. By spectrally resolving the emission, we could determine structure dependent field effects for many (n,m) species under identical conditions. In addition, the measured intensities represented averages over the distributions of nanotube lengths and angles to the electric field in the bulk sample and were therefore independent of these variables. Finally, the bulk approach allowed us to use a single excitation wavelength to generate photoluminescence from a range of (n,m) species in a single run. Figure 3 shows bulk emission spectra measured with and without external electric field.

As seen from Figure 3, at a fixed field of 2.3 V/μm, the photoluminescence peaks at shorter wavelengths experience weaker quenching than those at longer wavelength. This shows that photoluminescence of carbon nanotubes with smaller E_{11} transition energies (and larger diameters) is more sensitive to applied electric fields. In Figure 4a, we show quenching curves measured for five different (n,m) species in the film sample. These data could have deviated from the form of eq 1 because they represent averages over nanotube length and orientation. However, the small extent of quenching allows these ensemble averages to closely follow the functional form found for single nanotubes, as illustrated by the model fits in Figure 4a. Figure 4b displays the strong dependence of deduced quenching coefficient on optical band gap E_{11}. Although most of the SWCNTs in our sample were submicron in length, we performed limited measurements on longer nanotubes that had optically resolvable lengths of several microns. In these experiments, we found that longer

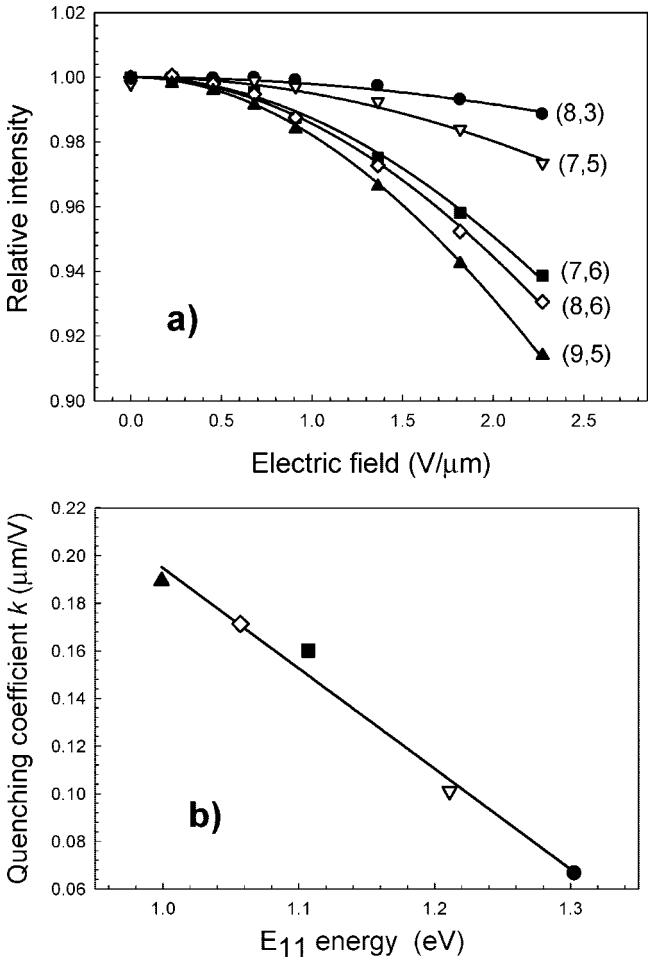

Figure 4. (a) Quenching data and model fits (based on eq 1) for five nanotube species. (b) Dependence of photoluminescence quenching coefficient on E_{11} transition energy. Data were measured using lamp excitation of bulk samples.

carbon nanotubes showed stronger quenching than shorter ones in the same applied field. A more detailed study of this phenomenon will be presented in a future report.

In deducing the quenching mechanism, we first exclude the electroabsorption effects described in recent papers, as they are much too weak to account for the observed fluorescence decrease.[18,19] Another possibility might be charge transfer between host and nanotube. However, our data were taken under conditions of no measurable current flow between electrodes. In addition, similar experiments in a host polymer more conducive to charge transfer revealed qualitatively different, time-dependent fluorescence changes. We therefore deduce that the quenching observed here is not from field-induced doping. An important clue to the mechanism is the inverse hyperbolic cosine dependence of intensity on field strength (eq 1). The denominator, which can be viewed as representing field-induced changes in nonradiative decay rate, contains the sum of two exponential terms. These terms vary in opposite ways with applied field: one increases the nonradiative decay from its zero-field value while the other decreases it. Thus, a possible interpretation is that the nonradiative decay is dominated by processes at the two axial falloff regions of the excitonic wave function. Computations indicate that the separation between these two "edges" (given by the exciton's spatial extent) is on the order of 3 nm.[24] Although the edge locations are equivalent in the absence of a field, they acquire different potential energies when the external field is applied, leading to an increase of electron density on one side and a decrease on the other. As a result of this polarization, one edge may give enhanced nonradiative decay, perhaps from exciton dissociation, while the other gives reduced decay. Because the relative electron densities should be described by Boltzmann factors involving the field, one can obtain the two terms in the denominator of eq 1, representing contributions from regions of extended and contracted excitonic electron wave function. The data in Figure 4b show that quenching occurs more readily in nanotubes with smaller band gaps, which are known to have smaller exciton binding energies. This observation is consistent with the model above if reduced binding energy allows greater field-induced electron density changes near the exciton edges.

Another interesting question is the influence of electric field on SWCNT optical transition energies. According to multiple predictions, transverse electric fields modulate SWCNT band gaps and give corresponding shifts in spectral transitions.[13,14,16,25] We investigated this possibility in our measurements, but found no detectable spectral shifts for transverse electric fields up to 20 V/μm. This negative result may be explained by the fact that the fields considered in theoretical predictions were substantially greater than could be applied in our apparatus.[13,14,16,25] Thus, it is likely that the field-induced spectral shifts were too small for these experiments to resolve. With longitudinal, rather than transverse, electric fields, we observed that some SWCNTs experienced small shifts on the order of $10-30$ cm^{-1}, while others did not display any consistent spectral shifts. Unfortunately, detailed studies of this phenomenon were prevented by the strong quenching of photoluminescence signals at the higher fields.

In conclusion, the influence of an external electric field on carbon nanotube photoluminescence has been observed and studied for the first time. Emission from SWCNTs embedded in PMMA dielectric matrixes was investigated using steady state fluorimetry for bulk samples and fluorescence microscopy for individual nanotubes. We found that photoluminescence intensity is decreased in an electric field and recovers when the field is removed. SWCNT photoluminescence intensity generally varies as the inverse hyperbolic cosine of the electric field magnitude multiplied by a single quenching coefficient. The quenching coefficient in turn varies approximately as the cosine of the angle between the electric field and the SWCNT axis, indicating that quenching is dominated by the electric field component along the nanotube axis. Moreover, the quenching coefficients depend strongly on nanotube structure, with smaller band gap species showing greater quenching coefficients. We present a simple quenching model intended to stimulate more rigorous theoretical research into the phenomena uncovered here. We expect that further investigations of field-induced quenching will lead to new insights into excitonic effects in

carbon nanotubes and an improved foundation for developing nanoscale optoelectronic devices.

Acknowledgment. This work was supported by grants from the NSF Center for Biological and Environmental Nanotechnology (EEC-0647452), the Welch Foundation (C-0807), and Applied NanoFluorescence, LLC. The authors are also grateful to S. W. Casscells, III, and J. L. Conyers (University of Texas Health Science Center, Houston) for instrumentation support. D.A.T. thanks the Welch Foundation for a postdoctoral fellowship (L-C-0004). We thank D. Natelson and J. Worne for expert assistance with gold deposition.

References

(1) Saito, R.; Dresselhaus, G.; Dresselhaus, M. S. *Physical Properties of Carbon Nanotubes*; Imperial College Press: London, 1998.
(2) Meyyappan, M., Ed.; *Carbon Nanotubes: Science and Applications*; CRC Press: Boca Raton, 2004.
(3) Collier, C. P. Carbon Nanotube Tips for Scanning Probe Microscopy. In *Carbon Nanotubes*, O'Connell, M. J., Ed.; CRC Press: Boca Raton, 2006; pp 295−313.
(4) Lim, S. C.; Lee, K.; Lee, I. H.; Lee, Y. H. *Nano* **2007**, *2*, 69–89.
(5) Chen, Y. C.; Raravikar, N. R.; Schadler, L. S.; Ajayan, P. M.; Zhao, Y. P.; Lu, T. M.; Wang, G. C.; Zhang, X. C. *Appl. Phys. Lett.* **2002**, *81*, 975–977.
(6) Martel, R.; Schmidt, T.; Shea, H. R.; Hertel, T.; Avouris, P. *Appl. Phys. Lett.* **1998**, *73*, 2447–2449.
(7) Tans, S. J.; Verschueren, A. R. M.; Dekker, C. *Nature* **1998**, *393*, 49–52.
(8) Avouris, P.; Radosavljevic, M.; Wind, S. J. Carbon Nanotube Electronics and Optoelectronics. In *Applied Physics of Carbon Nanotubes*, Rotkin, S. V., Subramoney, S., Eds.; Springer: Berlin, 2005; pp 227−251.
(9) Misewich, J. A.; Avouris, Ph.; Martel, R.; Tsang, J. C.; Heinze, S.; Tersoff, J. *Science* **2003**, *300*, 783–786.
(10) Kazaoui, S.; Minami, N.; Nalini, B.; Kim, Y.; Takada, N.; Hara, K. *Appl. Phys. Lett.* **2005**, *87*.
(11) Bachilo, S. M.; Strano, M. S.; Kittrell, C.; Hauge, R. H.; Smalley, R. E.; Weisman, R. B. *Science* **2002**, *298*, 2361–2366.
(12) Ohno, Y.; Kishimoto, S.; Mizutani, T. *Nanotechnology* **2006**, *17*, 549–555.
(13) O'Keeffe, J.; Wei, C. Y.; Cho, K. J. *Appl. Phys. Lett.* **2002**, *80*, 676–678.
(14) Pacheco, M.; Barticevic, Z.; Rocha, C. G.; Latge, A. *J. Phys.: Condens. Matter* **2005**, *17*, 5839–5847.
(15) Rocha, C. G.; Pacheco, M.; Barticevic, Z.; Latge, A. *Braz. J. Phys.* **2004**, *34*, 644–646.
(16) Novikov, D. S.; Levitov, L. S. *Phys. Rev. Lett.* **2006**, *96*, 036402−1036402−4.
(17) Perebeinos, V.; Avouris, P. *Nano Lett.* **2007**, *7*, 609–613.
(18) Kishida, H.; Nagasawa, Y.; Imamura, S.; Nakamura, A *Phys. Rev. Lett.* **2008**, *100*, 097401−1097401−4.
(19) Gadermaier, C.; Menna, E.; Meneghetti, M.; Kennedy, W. J.; Vardeny, Z. V.; Lanzani, G. *Nano Lett.* **2006**, *6*, 301–305.
(20) Nikolaev, P.; Bronikowski, M. J.; Bradley, R. K.; Rohmund, F.; Colbert, D. T.; Smith, K. A.; Smalley, R. E. *Chem. Phys. Lett.* **1999**, *313*, 91–97.
(21) Tsyboulski, D. A.; Bachilo, S. M.; Weisman, R. B. *Nano Lett.* **2005**, *5*, 975–979.
(22) Bachilo, S. M.; Strano, M. S.; Kittrell, C.; Hauge, R. H.; Smalley, R. E.; Weisman, R. B. *Science* **2002**, *298*, 2361–2366.
(23) Weisman, R. B.; Bachilo, S. M. *Nano Lett.* **2003**, *3*, 1235–1238.
(24) Capaz, R. B.; Spataru, C. D.; Ismail-Beigi, S.; Louie, S. G. *Phys. Rev. B* **2006**, *74*, 121401−1121401−4.
(25) Chen, R. B.; Lee, C. H.; Chang, C. P.; Lue, C. S.; Lin, M. F. *Physica E* **2006**, *34*, 670–673.

NL0800974